

# Optical Engineering

[SPIDigitalLibrary.org/oe](http://SPIDigitalLibrary.org/oe)

## **Fiber-optical grating sensors for wind turbine blades: a review**

Lars Glavind  
Ib Svend Olesen  
Bjarne Funch Skipper  
Martin Kristensen

# Fiber-optical grating sensors for wind turbine blades: a review

**Lars Glavind**

Aarhus University  
Department of Engineering  
Finlandsgade 22  
8200 Aarhus N, Denmark  
and  
Technology & Service Solutions  
Vestas Wind Systems A/S  
Hedeager 42  
8200 Aarhus N, Denmark  
E-mail: [lagla@vestas.com](mailto:lagla@vestas.com)

**Ib Svend Olesen**

Technology & Service Solutions  
Vestas Wind Systems A/S  
Hedeager 42  
8200 Aarhus N, Denmark

**Bjarne Funch Skipper**

Aarhus University  
Aarhus School of Engineering  
Dalgas Avenue 2  
8000 Aarhus C, Denmark

**Martin Kristensen**

Aarhus University  
Department of Engineering  
Finlandsgade 22  
8200 Aarhus N, Denmark

**Abstract.** With the rapid growth of wind turbines and focus on maintenance costs structural measurements are becoming essential. Fiber-optical sensors have physical properties that make them suitable for embedding in wind turbine blades, such as small size and immunity to electrical interferences. Fiber-optical grating sensors can be utilized to provide important information regarding strain, temperature, and curvature of the blades, which can be applied in condition-monitoring to detect fatigue failure and furthermore for optimization of the production from the wind turbine. We provide an overview of the current status and a discussion on research and implementation of fiber Bragg gratings and long-period gratings in wind turbine blade sensors. © The Authors. Published by SPIE under a Creative Commons Attribution 3.0 Unported License. Distribution or reproduction of this work in whole or in part requires full attribution of the original publication, including its DOI. [DOI: [10.1117/1.OE.52.3.030901](https://doi.org/10.1117/1.OE.52.3.030901)]

Subject terms: fiber optical sensors; gratings; fiber applications.

Paper 121553V received Oct. 26, 2012; revised manuscript received Feb. 15, 2013; accepted for publication Feb. 15, 2013; published online Mar. 6, 2013.

## 1 Introduction

Over the past few years wind turbines have become larger, and the forces acting on the wind turbine blades have increased, which leads to a higher possibility of fatigue failure of the wind turbines, such as broken wind turbine blades or tower strikes.<sup>1</sup> This causes the industry to have a high focus on condition monitoring of wind turbine components to reduce failure and maintenance costs by using active optimization of wind turbines based on wind turbine blade load sensors.<sup>1</sup> One method for condition-monitoring is to utilize structural measurement in the wind turbine blade based on either strain or bend sensors. Individual pitch control technology can then actively optimize the loads on the wind turbine blades and drive-train, without exceeding the safe limit, to prolong the operating lifetime.<sup>1</sup> A “cost-benefit” report regarding embedded load sensors in wind turbine blades, with a focus on the cost of damaged wind turbines and down-time has concluded that such a sensor system will have a cost break-even time of three to eight years depending on the cost of the sensor system.<sup>2</sup> Optimization, such as reduction of weight and increased power production, due to actively optimizing the wind turbine blade angle based on feedback from the sensor system, are not included in the “cost-benefit” report, and this will make the business-case even better.

For sensing in wind turbine blades, fiber-optical sensors are ideal. They have a small size for direct embedding with low risk of delamination,<sup>3</sup> multipoint sensors in the same fiber, good material compatibility for embedding with glass-fiber wind turbine blades.<sup>4</sup> Fiber-optical sensors are also nonconductive and immune to electrical interferences, which is of significant importance when embedded in wind turbine blades, due to the high risk of lightning. Without risk of corrosion, they are also more robust than conventional electrical sensors. Furthermore, fiber-optical grating sensors conduct a direct transformation of the sensed parameters to wavelengths, and are therefore normally independent of light levels, due to connector loss or changes in power from the light source. The sensors can either be applied to the wind turbine blade surface or be embedded into the wind turbine blade structure. As the signal is confined in low-loss optical fiber, signal reception and signal conditioning can be done away from the sensor, so putting any electrical parts in the wind turbine blade is avoided. This can, for example, be in the rotor hub (the part of the structure where the wind turbine blades and the main shaft are connected), which normally also contains electronic devices situated in a lightning-protected environment. Wireless transmission has been demonstrated between the signal-processing unit in the wind turbine rotor and the data handling system in the nacelle.<sup>5</sup>

illustrating the possibility for data transfer between the rotating and the stationary part of a wind turbine. However, there are also some disadvantages with fiber-optical sensors, such as thermal sensitivity, a limited number of suppliers and relatively high cost.<sup>6</sup> Other possibilities to control the wind turbines based on measurements can be using remote wind sensing, e.g., light detection and ranging (lidar),<sup>7</sup> where the wind speed is illuminated at a given distance in front of the wind turbine and analyzing is based on backscattering. However, this type of measurement does not provide the local data for strain or bend of the blade, and the systems are currently relatively expensive for use on single wind turbines. Fiber optical sensors based on grating technology are considered to be the most suitable sensors for wind turbine blades, and this paper treats the two most important grating technologies, fiber-Bragg gratings (FBGs) and long-period gratings (LPGs).

## 2 Fiber Bragg Gratings

### 2.1 Fiber Bragg Grating Introduction

An optical fiber grating consists of a periodic modulation of the properties of an optical fiber, typically changes in the refractive index of the core. Photosensitivity in optical fibers was discovered in 1978 by Hill et al.<sup>8</sup> In 1989 Meltz et al.<sup>9</sup> demonstrated the transverse writing of Bragg gratings. A considerable amount of literature has been published regarding fiber Bragg gratings such as Refs. 10 to 16. Phase-mask-based side-writing with ultraviolet (UV)-illumination is normally the preferred production method for FBGs.<sup>17</sup> The change in the refractive index is typically in the range up to  $1 \times 10^{-3}$ .<sup>13</sup> Germanium-doped fiber is most often used for inscribing FBGs due to high changes of refractive index.<sup>18</sup> To increase the photosensitivity of fibers, they are often loaded with hydrogen.<sup>19</sup>

Wavelengths that satisfy the Bragg conditions will be reflected<sup>13</sup>:

$$\lambda_B = 2n_{\text{eff}}\Lambda \quad (1)$$

where  $\lambda_B$  is the Bragg wavelength,  $n_{\text{eff}}$  is the effective refractive index of the fundamental mode and  $\Lambda$  is the spatial period of the grating. For the 1550-nm range the grating-period is typically in a range near 535 nm. FBGs typically have a total length near 5 mm.<sup>20</sup> Figure 1 shows an illustration of an FBG where broadband light is sent through the optical fiber, and the FBG reflects the Bragg wavelength  $\lambda_B$ .

For sensor applications the typical full width at half maximum (FWHM), for a FBG, is in the range of 0.05 to 0.3 nm.<sup>16</sup>

Figure 2 shows a measured reflection spectrum of a commercially available FBG, with a center-wavelength at 1551 nm and a FWHM of 0.2 nm.

Due to changes in the material and refractive index FBGs are sensitive to temperature and strain, providing the

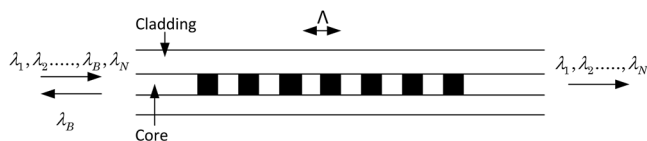


Fig. 1 Illustration of reflected light from an FBG.

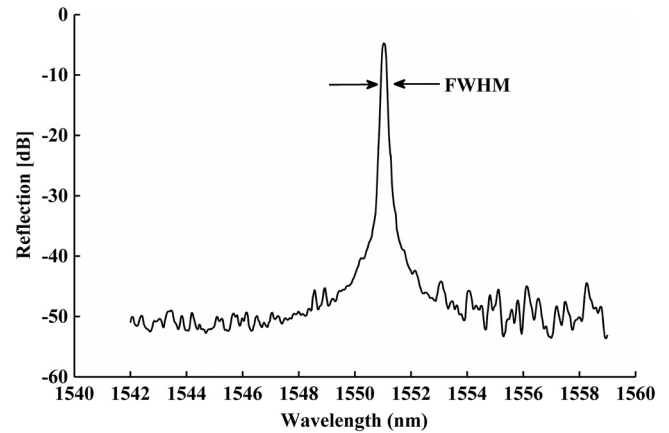


Fig. 2 Spectrum of an FBG.

possibility to be utilized as sensors. As the applied strain or temperature causes the center wavelength of the FBG to change, the number of consecutive FBGs along the same optical fiber will be limited by the grating FWHM, the induced strain and temperature wavelength tuning and the interrogator.

The strain sensitivity of FBGs is given by Ref. 13:

$$\Delta\lambda_B = (1 - p_e) \cdot \lambda_B \epsilon, \quad (2)$$

where  $\Delta\lambda_B$  is the change in Bragg wavelength,  $p_e$  is an effective strain-constant based on the strain-optic tensor and Poisson's ratio, with a typical value of 0.21,<sup>13</sup>  $\lambda_B$  is the given Bragg wavelength and  $\epsilon$  is the applied strain. For small longitudinal deformations ( $\delta \ll L_0$ ) the strain is defined as  $\epsilon = \delta/L_0$ , where  $\delta$  is the change in length, and  $L_0$  is original length.<sup>21</sup>

The temperature sensitivity of FBGs is given by Refs. 13 and 22:

$$\Delta\lambda_B = \lambda_B(\alpha + \xi)\Delta T, \quad (3)$$

where  $\alpha$  is the thermal expansion coefficient of the fiber, typically  $0.55 \times 10^{-6}$  m/(m · K), and  $\xi$  is the thermo-optic coefficient of the refractive index of the fiber, typically  $8.6 \times 10^{-6}$  K<sup>-1</sup>.<sup>13</sup> For a characteristic 1550-nm FBG this corresponds to a change of approximately 13.7 pm/K (depending on fiber composition).<sup>13</sup> Note that for a large temperature change the thermo-optic coefficient changes; however, within the expected operating temperatures for wind turbine sensors, 233 to 353 K (−40°C to 80°C), the coefficient can be assumed linear. Temperature drift can be reduced by utilizing material with opposite thermal expansion, such as zirconium tungstate,<sup>23</sup> for embedding. It is also possible to utilize the temperature-sensitivity of FBGs to measure the actual temperature with an extra FBG, which is mechanically decoupled, and use it to actively compensate for temperature drift in the control software.

### 2.2 Fiber-Bragg Gratings as Wind Turbine Load Sensors

FBGs utilized as wind turbine blade load sensors, based on strain measurements in wind turbine blades, have been published in several papers,<sup>1,3,5,24–28</sup> and the technology is

proven to be capable of measuring the maximum loads on wind turbine blades with the required resolution. Comparison of FBGs and standard electrical strain-gauges has been done on a small wind turbine blade. The experiment demonstrated that the Fourier spectrum of the strain gauges and the FBGs was similar. However, more resonance peaks were found in the Fourier spectrum of the FBGs.<sup>1</sup> This might indicate that it will be simpler to utilize FBGs to measure different resonance-modes of the wind turbine blades than with standard electrical strain-gauge. There is a requirement for 20 years operating lifetime for wind turbine blade sensors,<sup>26</sup> and the aspect of embedding the sensors in wind turbine blades is very important. Krebber et al.<sup>3</sup> demonstrated embedded FBG sensors in composite structures for wind turbine blades. The conclusion was that more research is required regarding an optimized coating to provide reliable measurement results. Furthermore, the grating reflectivity decays over time; however, it is possible to slow down the decay by an annealing treatment and ensure a lifetime of the required 20 years.<sup>29</sup> Studies have shown that the median breaking strain of an optical fiber is decreased from 57,000 to 27,000  $\mu\epsilon$  after UV exposure during writing of FBGs. Moreover, the optical fiber sensor still has a breaking strength sufficiently higher than the maximum strain measured in field tests,<sup>30</sup> in particular if great care is taken to avoid microscopic scratches/cracks in the fiber during cladding/stripping and re-coating/gluing. Furthermore, companies such as FBGS technologies<sup>31</sup> provide FBGs that are written during production of the optical fiber. This gives more robust fibers since the fiber is homogeneously coated, which decreases the possibility of a defect sensor due to tiny cracks from the removing of coating and imperfect re-coating.

FBG systems have been demonstrated in field tests, e.g., Schroeder et al.<sup>26</sup> Several companies such as Moog,<sup>32</sup> Fibersensing,<sup>33</sup> Smartfibers,<sup>34</sup> and HBM<sup>35</sup> provide commercial FBG sensing products for wind turbine blades, which typically are embedded on the inside surface of the wind turbine blade. These commercial systems sometimes offer resolutions down to 1  $\mu\epsilon$  with a typical dynamic range up to  $\pm 5000 \mu\epsilon$ . Furthermore, research studies regarding FBG utilized as impact response sensors on wind turbine blades have also been published.<sup>4</sup> Detection systems for FBGs are relatively expensive, since a wavelength range of up to 50 nm, with a resolution in the range of 1 pm, needs to be interrogated. This is most easily performed with a tunable narrow-band source and a photo-diode or a combination of a broadband light source and a spectrometer. However, a potentially cheaper solution is detection based on wavelength division (de)-multiplexing (WDM) filters. Such transceivers are commercially available from, for example, Redondo Optics.<sup>36</sup> This detection technique has also been demonstrated to meet high-resolution demand for use in wind turbine applications.<sup>37</sup>

Another possibility to measure the loads on a wind turbine blade is utilization of a sensor that is capable of measuring the curvature of the wind turbine blade. Strain in the wind turbine blade from the wind makes the wind turbine blade bend. Therefore, it might be better to measure the curvature of the wind turbine blade directly. FBGs have also been demonstrated as bending sensors with a sensitivity of  $0.77 \times 10^{-12} \text{ m}^2$ .<sup>38</sup> This type of utilization of FBGs has

not yet, to our knowledge, been implemented in wind turbine applications. Bend sensors in polymer optical fibers based on FBGs have been demonstrated by Chen et al.<sup>39,40</sup> However, polymer optical fibers are more fragile and sensitive to mechanical exhaustion than typical silica optical fibers, and therefore they are not preferred for applications in wind turbines.

### 2.3 Discussion of Bragg Sensors for Wind Turbines

FBG strain sensors for structural monitoring on wind turbine blades is a mature and highly developed technique. Commercial systems typically provide a strain resolution of 1  $\mu\epsilon$  with a dynamic range of  $\pm 5000 \mu\epsilon$  for structural information about wind turbine blades. Multiple sensors in the same fiber are possible, and thereby utilization for control applications, typically requiring two to six sensors, and for supervision application, typically requiring eight to 16 sensors, is achievable. The technique can provide the required lifetime of 20 years for the sensors utilized in wind turbine blades.<sup>29</sup> The concept has been demonstrated in field tests, and FBG strain sensing systems are commercially available specific for wind turbine applications. A typical application is measurements of strain in the root, where the sensors are placed in the circumference of the blade-root, and the sensors are orientated in the longitudinal direction. By mounting more than one sensor cylindrically in the wind turbine blade, the sensors can also provide edge-wise and flapwise strain sensing. These requirements can be provided by commercially available systems as mentioned above.

## 3 Long Period Gratings

### 3.1 Long-Period Grating Introduction

In the literature, the work by Vengsarkar et al.<sup>41,42</sup> is typically referred to as one of the first demonstrations of coupling from the fundamental-guided mode, in a single-mode fiber, to forward-propagating cladding modes, utilizing long-period gratings (LPG). However, before this paper, several studies of related functionality were performed, e.g., blazed grating in a two-mode fiber to induce  $LP_{01} \leftrightarrow LPG_{11}$  mode conversion,<sup>43</sup> and in fact, the basic ideas were originally demonstrated in microwave engineering many years ago.<sup>44</sup> A large amount of literature regarding LPGs has been published such as Refs. 14, 15, 42, 45, and 46. LPGs have spatial periods in the range of 100 to 500  $\mu\text{m}$ , which is approximately a factor 1000 larger than FBGs. LPGs have a typical length in the region of 30 mm.<sup>20</sup> LPGs couple light from the fundamental-core mode in a single-mode optical fiber into modes confined to the cladding (cladding modes). Figure 3 illustrates the electrical field distribution before and after an LPG.

The cladding-modes propagate in the same direction as the fundamental core mode, which is different compared

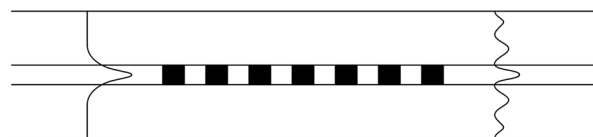


Fig. 3 Illustration of field distribution before and after an LPG.

to FBGs where the light is reflected at the grating. Compared to FBGs it is therefore only possible to interrogate the signal in the transmission end of the fiber. Therefore, for an embedded sensor in a wind turbine blade, it is required that the optical fiber is returned to the rotor hub for interrogation of the transmitted signal.

A part of the cladding-mode field penetrates through the external boundary, and cladding modes are sensitive to the surrounding of the optical fiber. The refractive index of the coating is typically higher than the refractive index of the cladding (cladding-mode stripping coating). Therefore, there is only partial reflection at the cladding-coating boundary. For cladding modes to persist, it is needed to have a refractive index-change, preferably a drop, at the cladding-to-coating boundary to ensure total reflection, i.e., the refractive index of the coating is lower than the refractive index of the cladding. For cladding modes with an incidence angle at the cladding-coating boundary, which is below the critical angle, the cladding-mode power will slowly diminish due to the radiation leakage into the polymer coating, where the radiation is soon absorbed or scattered,<sup>47</sup> so the imaginary part of the propagation-constant in the coating material cannot be ignored compared to the real part and the coupling strength of the LPG.

For LPGs, the phase-matching condition causes light from the fundamental guided mode to couple to forward-propagating cladding modes at distinct wavelengths given by Ref. 48:

$$\lambda^{(m)} = [n_{\text{eff}} - n_{\text{cl}}^{(m)}]\Lambda, \quad (4)$$

where  $n_{\text{eff}}$  is the effective index of the guided mode,  $n_{\text{cl}}^{(m)}$  is the refractive index of an azimuthally symmetric cladding mode of order  $m$  (for unblazed gratings), and  $\Lambda$  is the spatial grating period. (The asymmetric modes can also, to some smaller degree, be excited).

LPGs can be produced with several different methods, such as amplitude-modulated UV illumination,<sup>42</sup> mechanical pressure from plates,<sup>49</sup> acoustically induced micro-bending,<sup>50</sup> and splice-based controlled arc.<sup>51</sup> Because of the larger period, LPGs have the advantages that the demand for accuracy in production of LPGs is less critical, compared to FBGs' production.

The spectra from transmission-gratings can be calculated by the piecewise uniform approach based on  $2 \times 2$  matrices for each uniform section of the grating, where the grating is divided in  $M$  uniform sections of grating<sup>15</sup> (typically  $M \sim 10$  to 1000). For transmission gratings  $F_i$  (in the literature  $R$  is typically used; however, it is easily confused with  $R$  referring to reflection) is the fundamental mode amplitude and  $S_i$  is a different mode traveling in same direction. For transmission gratings the start is  $F_0 = F(-L/2) = 1$  and  $S_0 = S(-L/2) = 0$ ,  $L$  is the length of the grating, and calculated to  $F(L/2) = F_M$  and  $S(L/2) = S_M$ .  $P_{\text{in}}$  is input power of the fundamental mode. Figure 4 illustrates the definitions for transmission gratings.

The propagation through each uniform section  $i$  is described by a matrix  $T_i$  defined as:

$$\begin{bmatrix} F_i \\ S_i \end{bmatrix} = T_i \begin{bmatrix} F_{i-1} \\ S_{i-1} \end{bmatrix}. \quad (5)$$

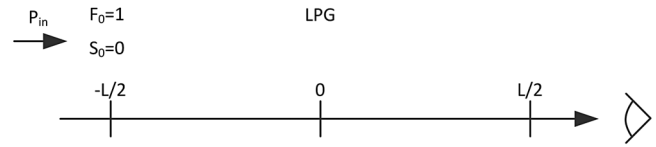


Fig. 4 Illustration of definitions of  $F_0$  and  $S_0$  for an LPG.

For LPGs the matrix is given by Refs. 13 and 15:

$$T_i = \begin{bmatrix} \cos(\gamma_c \Delta z) + i \frac{\hat{\sigma}}{\gamma_c} \sin(\gamma_c \Delta z) & i \frac{\kappa}{\gamma_c} \sin(\gamma_c \Delta z) \\ i \frac{\kappa}{\gamma_c} \sin(\gamma_c \Delta z) & \cos(\gamma_c \Delta z) - i \frac{\hat{\sigma}}{\gamma_c} \sin(\gamma_c \Delta z) \end{bmatrix}, \quad (6)$$

where  $\gamma_c \equiv \sqrt{\kappa^2 + \hat{\sigma}^2}$ ,  $\hat{\sigma}$  is a ‘‘DC’’ self-coupling (period-averaged) coupling coefficient,  $\kappa$  is an ‘‘AC’’ cross-coupling coefficient and are the local values in the  $i$ 'th section and  $\Delta z$  is the length of the  $i$ 'th section. Once all matrices for the individual sections are known, the output amplitudes can be calculated by:

$$\begin{bmatrix} F_M \\ S_M \end{bmatrix} = T \begin{bmatrix} F_0 \\ S_0 \end{bmatrix}; \quad T = T_M \cdot T_{M-1} \cdot \dots \cdot T_i \cdot \dots \cdot T_1. \quad (7)$$

More details regarding simulations of gratings can be found in work conducted by Erdogan.<sup>14,15</sup>

Figure 5 shows a measurement of the transmission spectrum for a typical commercially available LPG, with a center wavelength of 1532 nm and a FWHM of 19 nm.

The FWHM is typically larger than for FBGs, caused by the limited number of cascaded grating lines in one fiber sensor compared to the number for FBGs. Since the resonance wavelength depends on the difference between the core and cladding index, LPGs are more wavelength-sensitive to the decay of grating strength.<sup>52</sup> Accelerated aging experiments have demonstrated that over a predicted lifetime of 25 years, the center wavelength can change  $<0.02$  nm at 313 K (40°C) and  $<0.12$  nm at 333 K (60°C).<sup>52</sup> In the design for a given application and temperature environment, this must be taken into consideration, for example, by running calibrations. More research regarding lifetime for wind turbine blade applications is therefore required to ensure that LPG sensors are suitable for wind turbine applications.

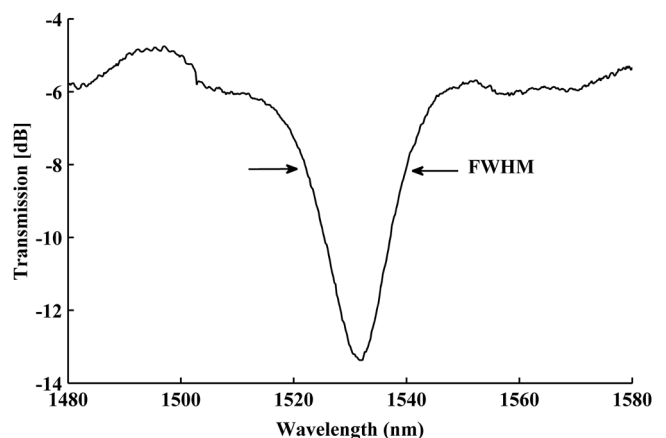


Fig. 5 Spectrum from an LPG.

### 3.2 Long-Period Temperature Sensitivity

LPGs are sensitive to temperature and strain due to changes in the fundamental and the cladding modes' effective refractive indices and the change in grating period. Using the chain rule of derivatives, the sensitivity to temperature can be obtained from Eq. (7) as Ref. 48:

$$\frac{d\lambda}{dT} = \frac{d\lambda}{d(\delta n_{\text{eff}})} \left( \frac{dn_{\text{eff}}}{dT} - \frac{dn_{\text{cl}}}{dT} \right) + \Lambda \frac{d\lambda}{d\Lambda} \frac{1}{L} \frac{dL}{dT}, \quad (8)$$

where  $\lambda$  is the center wavelength of the attenuation band,  $T$  is the temperature,  $n_{\text{eff}}$  is the effective refractive index of the fundamental mode,  $n_{\text{cl}}$  is the effective refractive index of the cladding mode,  $\delta n_{\text{eff}} = (n_{\text{eff}} - n_{\text{cl}})$ ,  $L$  is the length of the LPG and  $\Lambda$  is the period of the LPG. The first term on the right-hand side is the material contribution and is related to the change in the differential refractive index of the core and cladding arising from the thermo-optic effects. The second term is the waveguide contribution as it results from changes in the period. With an appropriate selection of fiber composition and grating period, it is possible to balance the two contributions and suppress temperature drift for an LPG sensor. For unbalanced LPGs in optical fibers, the typical temperature sensitivity is in the range of 5 to 15 nm/100 K;<sup>53</sup> however, it depends on the fiber composition and grating period.

Since the center wavelength is dependent on the refractive index of the coating material, it is possible to utilize the coating material for temperature compensation. LPGs in typical germanium-doped silica core fiber have a red shift  $d\lambda/dT$  due to positive  $d(n_{\text{eff}} - n_{\text{cl}})/dT$ . The temperature drift can be compensated by selecting a coating material that has an increase in refractive index as the temperature increases. However, conventional polymer for recoating has a generally negative  $dn/dT$ . It is possible to design the optical fiber to have a blue shift  $d\lambda/dT$  by germanium/boron co-doping. This has been utilized to design a balanced LPG, where the temperature drift is suppressed to +0.07 nm/100 K, compared to a typically unbalanced LPG with 5 to 15 nm/100 K.<sup>53</sup>

### 3.3 Long-Period Strain Sensitivity

The sensitivity for a LPG due to axial strain is given by Ref. 48:

$$\frac{d\lambda}{d\varepsilon} = \frac{d\lambda}{d(\delta n_{\text{eff}})} \left( \frac{dn_{\text{eff}}}{d\varepsilon} - \frac{dn_{\text{cl}}}{d\varepsilon} \right) + \Lambda \frac{d\lambda}{d\Lambda}. \quad (9)$$

The first and second terms on the right-hand side are termed material and waveguide contributions. The material contribution results from the strain optics (change in refractive index) and Poisson's effect (change in transverse dimensions), while the waveguide contribution depends on the slope  $d\lambda/d\Lambda$  of the characteristic curve of the resonance band. Typically, for an LPG with  $\Lambda > 100 \mu\text{m}$ , the material contribution is negative, while the waveguide contribution is positive. For  $\Lambda < 100 \mu\text{m}$  both contributions to the strain sensitivity are negative.<sup>20,48</sup> For example, Bhatia et al. have demonstrated strain sensitivity for LPGs of 0.04 pm/ $\mu\varepsilon$  and -2.2 pm/ $\mu\varepsilon$  with different grating periods.<sup>48</sup> Selecting an appropriate periodicity and fiber composition for LPGs gives the possibility of designing the sensor strain-sensitive

or insensitive, if the material and waveguide contributions are equal but with opposite sign. LPGs can measure strain and temperature with an optical spectral sensitivity almost an order-of-magnitude higher than FBGs,<sup>42</sup> giving the possibility of utilizing it as strain or temperature sensor.<sup>54</sup> However, LPGs typically have large spectral widths, compared to FBGs, which limits the effective resolution. For the given applications, such as measuring on wind turbine blades, the composition of the fiber and the order of the cladding mode must be taken into account in the design of the sensor to suppress or increase temperature and/or strain sensitivity sufficiently for the given application.

### 3.4 Long-Period Gratings as Bend Sensors

In 1998 LPGs were investigated as bend sensors, and a bend direction asymmetry was observed for the resonance wavelength shift in one direction.<sup>55,56</sup> Based on this, it is possible with a combination of two or more LPGs to construct a bend-sensor to measure both the direction and magnitude of a bend.<sup>57</sup>

When an LPG is bending, new dips in the spectrum appear.<sup>58,59</sup> The new dip in the transmission band is significantly weaker and is typically about 10 nm shifted from the original dip. The wavelength separation of the split attenuation bands increases with bend curvature.<sup>59</sup> The splitting depends on the effective refractive index difference of the cladding modes and not on the difference between the refractive index of the core and cladding mode. Therefore, the sensor will not be affected by (to first order) cross-sensitivity to temperature, strain, and refractive index changes.<sup>60</sup> Under temperature drift, the wavelength distance between the two dips will therefore not change (to first order), only the absolute wavelength of both dips will change.<sup>61</sup>

Figure 6 shows the principle of splitting in the transmission spectra when an LPG is bending. Dip 1 is the original transmission dip and dip 2 is the new dip.

Several papers<sup>61-63</sup> have explained the splitting by stating that the fiber-curvature breaks the degeneracy of the cladding modes that are normally coupled to in the straight fiber. These nondegenerate modes, with power concentrated on opposite sides of the fiber core, then propagate with different speeds due to the difference in longitudinal strain above and below the fiber axis.

However, using numerical modeling, Block et al.<sup>64</sup> analyzed modes of a curved three-layer optical fiber. They found that the splitting is caused by asymmetric changes of the effective indices of the cladding modes and the core mode,

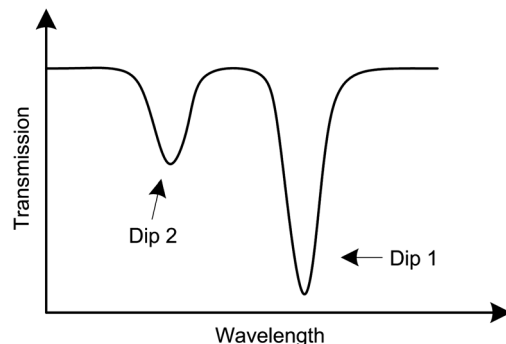


Fig. 6 Splitting of LPG dips.

which breaks the cladding-mode symmetry. This explains why the original attenuation notches, present in the straight fiber, shift in wavelength as curvature is increased. Allowing coupling to cladding modes with higher order azimuthal symmetry than allowed in a straight fiber, which results in new notches at nearby wavelengths. Furthermore, it has been experimentally demonstrated that the strengths and the positions show no significant polarization dependence.<sup>58</sup>

### 3.5 Long Period Gratings as Directional Bend Sensor

If the geometry of the fiber is designed such that the core is not symmetrically in the center of the fiber, the splitting of dips occur without bending of the LPG.<sup>60,65</sup> Rathje et al. in 1999, used an optical fiber with core concentricity error (CCE) of  $2.4 \mu\text{m}$  to demonstrate a direction-sensitive fiber-optical bend sensor based on LPGs.<sup>60,65</sup> Patrick<sup>66</sup> showed that to maximize the bending sensitivity the CCE can be increased, where an optical fiber with a CCE of  $14 \mu\text{m}$  was demonstrated. A too large CCE, however, can give limitations regarding dynamic range for a given application. The changes in splitting and the amplitude of the curvature are approximately linear, but with curvature around  $0 \text{ m}^{-1}$  the sensitivity is lower.<sup>67</sup> This needs to be taken into consideration for the design of a given sensor.

The direction of the CCE can be determined with light diffraction.<sup>67,68</sup> For production and embedding into wind turbine blades, this method, to align the sensor correctly, demands high precision and is therefore time consuming. Furthermore, typical methods for production of optical fibers are optimized to avoid CCE (minimize CCE), and a fiber with a specific CCE for sensor use needs to be a special production.

Other fibers where the core is not located in the center of the cladding, such as D-shaped and multicore fibers, or where the index profile is not symmetrical around the core, also provide useful bend and direction sensing. This has, for example, been shown in D-shaped fibers.<sup>69,70</sup> Zhao et al. has demonstrated bend sensing in four-core fiber, D-shaped, and flat-clad fiber.<sup>71</sup> These fiber types, where the cladding is flat, are easier to handle during embedding than optical fibers with CCE. The flat side of the fiber can be aligned on a base-plate giving an easier way to orientate the bend-direction sensitive sensor. They are therefore less time consuming in the embedding process for the wind turbine blade, and the risk for error placing the sensors is decreased. Furthermore, these fibers have been commercially available<sup>71</sup> and are more distributed than CCE fibers. In addition, D-shaped fiber has the advantage that it can be produced by more or less existing standard optical fiber production methods.

Bend sensors based on LPGs have not yet, to our knowledge, been implemented into wind turbine blades and are not investigated as deeply as FBGs for this application, leaving a number of uncertainties regarding the possibilities to utilize D-shaped or other asymmetric fiber LPGs for turbine blade load sensors. The required resolution and cascade coupling of sensors in the same fiber are still unknown. However, LPG sensors have been implemented in other structures, such as bonded to the surface of a steel plate using an unsaturated polyester adhesive.<sup>59</sup> and embedded in capillaries structures,<sup>72</sup> indicating some possibility for embedding the sensor in wind turbine blades.

### 3.6 Direct Embedding of Long Period Grating Sensors

We have conducted initial research regarding direct embedding of LPGs into a wind turbine blade. The LPGs have been embedded by use of the standard adhesive utilized in wind turbine blade production by the wind turbine manufacturer Vestas Wind Systems A/S for modern turbines.

The fibers were embedded with the adhesive onto a fiber-glass base-plate, and the adhesive was cured using normal procedure. Figure 7 shows the spectra of an LPG without coating before and after embedding. It is clearly seen that the spectrum is broadened and shifted, and the dip is decreased from about 12 to 3.5 dB. In addition, the FWHM is increased from 12 nm to approximately 25 nm. Figure 8 shows the spectra of a recoated LPG, refractive index of 1.375, before and after embedding with the same type of adhesive. The recoating must be done with care to provide an even coating along the fiber. With recoating, the dip is only decreased from 6.4 to 5 dB, and there is no significant broadening. The shift is also smaller. Moreover, the shift is mainly due to the prestress applied to ensure the fiber is straight. The refractive index from the adhesive is expected to have the most influence on the broadening of the spectra; however, micro-bend and stress might also have an influence and are subjects for further investigation.

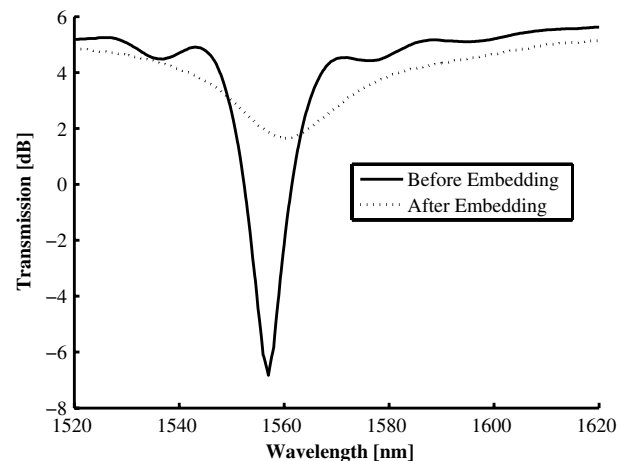


Fig. 7 LPG embedded without recoating.

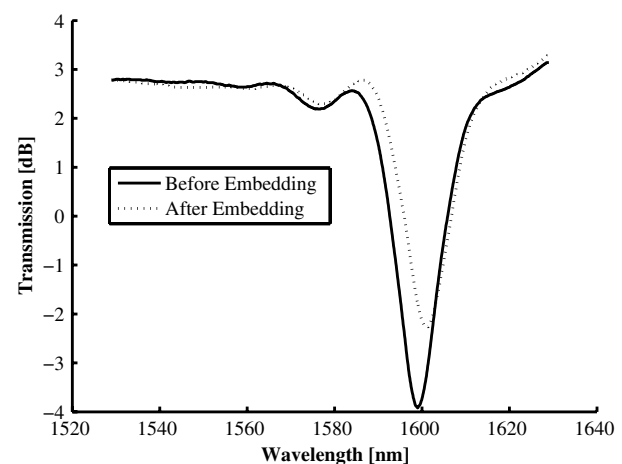


Fig. 8 LPG embedded with low refractive coating.

The experiment demonstrates that without recoating, the dip is broadened and is not sufficiently deep and narrow for sensing. Moreover with proper recoating the dip is adequate to be utilized as a sensor. The experiments demonstrate the possibility for direct embedding of LPG sensors implemented in the manufacturing-process of wind turbine blades.

### 3.7 Discussion of Long-Period Grating Sensors for Wind Turbines

Bend sensors based on LPGs offer another type of load sensor than the typical ones based on FBGs. However, the LPG technology is not so mature for utilization in wind turbine blade load sensors as the FBG technology. More research needs to be performed for determination of the best parameters to achieve optimized design and correct embedding. Our estimates, based on typical wind turbine blade curvature for modern wind turbine blades (>50 m), acceptable resolution, and commercially available detection systems, gives a minimum required resolution of the sensor system in the range of the resolution of the  $12.55 \times 10^{-9} \text{ m}^2$  as demonstrated by Allsop et al.<sup>69</sup> Compared to the bend resolution for an FBG,  $0.77 \times 10^{-12} \text{ m}^2$ ,<sup>38</sup> the bend sensitivity for LPGs is much higher. Furthermore, the required resolution of the sensor and the corresponding detection system needs to be investigated to verify that the sensor can be utilized to actively optimize a wind turbine. The design depends on wind turbine blade parameters such as length, material stiffness, and physical design. LPGs differ from FBGs by having a much longer period and having cladding modes that depend on the refractive index of the medium (coating) surrounding the optical fiber. Therefore, the materials for embedding LPG sensors might be different from the materials used for FBG sensors. For example, nonuniform strain in the adhesive, used for attaching the fiber to the wind turbine blade, might act differently on LPG sensors than on FBG sensors, as indicated from our initial experiments. LPGs offer, with the correct geometry of the optical fiber, such as CCE or D-shape, the possibility to passively out-compensate temperature and strain-drift through the design of the optical fiber, where no extra temperature sensors or special materials for embedding are required. Extensive research and development is required to develop an LPG bend sensor into an alternative sensor system that is competitive with commercially available FBG sensor systems. Moreover, the LPG bend sensor has the possibility to offer a new type of sensor that can measure the bend directly, which might be a more natural method of sensing the shape of and the load on the wind turbine blade. This may be exploited to give better performance of the wind turbine based on active optimization.

Much research has been done on utilizing fiber optical grating sensors for structural health monitoring on other structures such as aircrafts,<sup>73</sup> bridges,<sup>74</sup> and trains.<sup>75</sup> This is typically based on strain measurement with FBGs. Moreover, compared to wind turbine applications, the bends of these structures are significantly smaller than the bend of the wind turbine blade. Therefore the benefit of utilizing LPGs as bend sensors for applications, such as aircrafts, bridges and trains, do not have the same prospective as with wind turbine blade applications. Here, the structural deformations are large enough to overcome the issues regarding large spectral width of the LPGs. For LPG sensors,

similar performance regarding operating temperature range and lifetime as for FBGs is expected, as well as the number of sensors.

## 4 Combined Sensors

Combined strain and temperature measurement with FBGs has been demonstrated.<sup>76,77</sup> Combined temperature and bend/curvature measurement with LPGs has also been demonstrated.<sup>78,79</sup> With both bend, strain, and temperature measurement, the prediction of the wind turbine blade condition over time is more accurate. The next generation of load sensors is likely to be such a type of combined sensors.

## 5 Conclusion

Fiber-optical grating sensors have advantages that make them suitable as load sensors in wind turbine blades. Most research and development have been concentrated on the utilization of FBGs as wind turbine blade load sensors based on the measurement of strain, which is actively temperature compensated. The technology is mature and commercial systems are available. Since strain in a wind turbine blade predominantly arises from bending of the wind turbine blade, it might be natural to measure the bend directly. Sensors based on LPGs offer this type of load sensor, where it is possible to measure the bend of the wind turbine blade directly. Furthermore, passive temperature and strain compensation is possible within LPG bend sensors through the geometrical design of the optical fiber. Investigations regarding the specifications that are needed for a bend sensor to be utilized as a sensor for active optimizing of wind turbines are required. Research regarding design of the sensor to achieve the needed resolution and embedding in wind turbine blades is under way. This includes parameters of the fiber, embedding materials, and physical placement in the wind turbine blades. Our initial research regarding LPGs in wind turbine blades indicates the possibility for direct embedding into the blades. Moreover, with this research done, it is believed that it is possible to provide a new type of sensor that can measure a profile of the loads on a wind turbine blade based on curvature measurements.

### Acknowledgments

The authors thank Vestas Wind Systems A/S for funding this review of fiber-optical grating sensors for wind turbine blades. The authors thank, optic specialist at Vestas Wind Systems A/S, Heidi M. Hyldahl, for proofreading the manuscript.

### References

1. K. Chang-Hwan, P. Insu, and Y. Neungsoo, "Monitoring of small wind turbine blade using FBG sensors," in *2010 Int. Conf. Control Automation and Systems (ICCAS)*, pp. 1059–1061, IEEE, New York, NY (2010).
2. L. G. Hansen and L. Lading, "Fundamentals for remote structural health monitoring of wind turbine blades—a preproject. Annex A. Cost-benefit for embedded sensors in large wind turbine blades," Risø National Laboratory, p. 37, ISBN: 87-550-3045-9 (2002).
3. K. Krebber et al., "Fiber Bragg grating sensors for monitoring of wind turbine blades," *Proc. SPIE* **5855**, 1036–1039 (2005).
4. C. S. Shin et al., "Impact response of a wind turbine blade measured by distributed fbG sensors," *Mater. Manuf. Process.* **25**(4), 268–271 (2010).
5. W. Ecke and K. Schroeder, "Fiber Bragg grating sensor system for operational load monitoring of wind turbine blades," *Proc. SPIE* **6933**, 69330I (2008).
6. A. Méndez, "Fiber Bragg grating sensors: a market overview," *Proc. SPIE* **6619**, 661905 (2007).

7. T. Mikkelsen et al., "Lidar wind speed measurements from a rotating spinner," in *EWEC 2010 Conf. Proc.*, European Wind Energy Association, Brussels, Belgium (2010).
8. K. O. Hill et al., "Photosensitivity in optical fiber waveguides—application to reflection filter fabrication," *Appl. Phys. Lett.* **32**(10), 647–649 (1978).
9. G. Meltz, W. W. Morey, and W. H. Glenn, "Formation of Bragg gratings in optical fibers by a transverse holographic method," *Opt. Lett.* **14**(15), 823–825 (1989).
10. M. Yamada and K. Sakuda, "Analysis of almost-periodic distributed feedback slab waveguides via a fundamental matrix approach," *Appl. Opt.* **26**(16), 3474–3478 (1987).
11. K. O. Hill and G. Meltz, "Fiber Bragg grating technology fundamentals and overview," *J. Lightwave Technol.* **15**(8), 1263–1276 (1997).
12. R. Kashyap, *Fiber Bragg Gratings*, Academic Press, Burlington, MAQ (2009).
13. A. Othonos and K. Kalli, *Fiber Bragg Gratings: Fundamentals and Applications in Telecommunications and Sensing*, Artech House Publisher, Norwood, MA (1999).
14. T. Erdogan, "Cladding-mode resonances in short- and long-period fiber grating filters," *J. Opt. Soc. Am. A* **14**(8), 1760–1773 (1997).
15. T. Erdogan, "Fiber grating spectra," *J. Lightwave Technol.* **15**(8), 1277–1294 (1997).
16. A. D. Kersey et al., "Fiber grating sensors," *J. Lightwave Technol.* **15**(8), 1442–1463 (1997).
17. K. O. Hill et al., "Bragg gratings fabricated in monomode photosensitive optical fiber by UV exposure through a phase mask," *Appl. Phys. Lett.* **62**(10), 1035–1037 (1993).
18. M. Kristensen, "Ultraviolet-light-induced processes in germanium-doped silica," *Phys. Rev. B* **64**(14), 144201 (2001).
19. P. J. Lemaire et al., "High pressure H<sub>2</sub> loading as a technique for achieving ultrahigh UV photosensitivity and thermal sensitivity in GeO<sub>2</sub> doped optical fibres," *Electron. Lett.* **29**(13), 1191–1193 (1993).
20. S. W. James and R. P. Tatam, "Optical fibre long-period grating sensors: characteristics and application," *Meas. Sci. Technol.* **14**(5), R49 (2003).
21. C. Nordling and J. Österman, "Solid Mechanics," in *Physics Handbook for Science and Engineering*, p. 369, Studentlitteratur, Lund, Sverige (2004).
22. G. Meltz and W. W. Morey, "Bragg grating formation and germano-silicate fiber photosensitivity," *Proc. SPIE* **1516**, 185–199 (1991).
23. A. W. Sleight, "Isotropic negative thermal expansion," *Annu. Rev. Mater. Sci.* **28**, 29–43 (1998).
24. S. Park, T. Park, and K. Han, "Real-time monitoring of composite wind turbine blades using fiber Bragg grating sensors," *Adv. Compos. Mater.* **20**(1), 39–51 (2011).
25. K. Schroder et al., "Fibre Bragg grating sensor system monitors operational load in a wind turbine rotor blade," *Proc. SPIE* **5855**, 270–273 (2005).
26. K. Schroeder et al., "A fibre Bragg grating sensor system monitors operational load in a wind turbine rotor blade," *Meas. Sci. Technol.* **17**(5), 1167–1172 (2006).
27. Z. Guo et al., "Structural health monitoring of composite wind blades by fiber bragg grating—art. no. 64230I," *Proc. SPIE* **6423**, 64230I (2007).
28. H. Bang, H. Shin, and Y. Ju, "Structural health monitoring of a composite wind turbine blade using fiber Bragg grating sensors," *Proc. SPIE* **7647**, 76474H (2010).
29. D. L. Williams and R. P. Smith, "Accelerated lifetime tests on UV written intracore gratings in boron germania codoped silica fiber," *Electron. Lett.* **31**(24), 2120–2121 (1995).
30. H. G. Limberger et al., "Mechanical degradation of optical fibers induced by UV light," *Proc. SPIE* **2841**, 84–93 (1996).
31. FBGS, "FBGS—Draw Tower Gratings," <http://www.fbgs.com/> (4 March 2013).
32. MOOG, "Wind Energy—Wind Energy | Moog," <http://www.moog.co.uk/markets-overview/wind-energy/> (4 March 2013).
33. Fibersensing, "Fibersensing—Bringing light to measurement," <http://w3.fibersensing.com/> (4 March 2013).
34. Smart Fibres, "Smart Fibres. Optical Fibre Sensing with Fibre Bragg gratings (FBG) for process optimisation and condition monitoring: SMART FIBRES," <http://www.smartfibres.com/> (4 March 2013).
35. HBM, "HBM Test and Measurement: Transducer, Load Cell, DAQ," <http://hbm.com/> (4 March 2013).
36. Redondo Optics, "Redondo Optics," <http://www.redondooptics.com/> (4 March 2013).
37. L. Glavind et al., "Low-cost, high-resolution strain sensor for wind turbine applications," in *Bragg Gratings, Photosensitivity, and Poling in Glass Waveguides*, Optical Society of America, Washington, DC, paper JThA36 (2010).
38. A. Martinez et al., "Vector bending sensors based on fibre Bragg gratings inscribed by infrared femtosecond laser," *Electron. Lett.* **41**(8), 472–474 (2005).
39. X. Chen et al., "Highly sensitive bend sensor based on Bragg grating in eccentric core polymer fiber," *IEEE Photonics Technol. Lett.* **22**(11), 850–852 (2010).
40. X. Chen et al., "Optical bend sensor for vector curvature measurement based on Bragg grating in eccentric core polymer optical fibre," *Proc. SPIE* **7503**, 750327 (2009).
41. A. M. Vengsarkar et al., "Long-period fiber gratings as band-rejection filters," *J. Lightwave Technol.* **14**(1), 58–65 (1996).
42. V. Bhatia and A. M. Vengsarkar, "Optical fiber long-period grating sensors," *Opt. Lett.* **21**(9), 692–694 (1996).
43. K. Hill et al., "Efficient mode conversion in telecommunication fiber using externally written gratings," *Electron. Lett.* **26**(16), 1270–1272 (1990).
44. S. Miller and W. Mumford, "Multi-element directional couplers," *Proc. Institute of Radio Eng.* **40**(9), 1071–1078 (1952).
45. J. Rathje, "Thermal stability and practical applications of UV induced index changes in silica glasses," Ph.D. Thesis (Technical University of Denmark, Department of Communications, 2000).
46. Y. Liu et al., "Optical bend sensor based on measurement of resonance mode splitting of long-period fiber grating," *IEEE Photonics Technol. Lett.* **12**(5), 531–533 (2000).
47. O. V. Ivanov, S. A. Nikitov, and Y. V. Gulyaev, "Cladding modes of optical fibers: properties and applications," *Physics-Uspekhi* **49**(2), 167–191 (2006).
48. V. Bhatia et al., "Temperature-insensitive and strain-insensitive long-period grating sensors for smart structures," *Opt. Eng.* **36**(7), 1872–1876 (1997).
49. S. Savin et al., "Tunable mechanically induced long-period fiber gratings," *Opt. Lett.* **25**(10), 710–712 (2000).
50. H. S. Kim et al., "All-fiber acousto-optic tunable notch filter with electronically controllable spectral profile," *Opt. Lett.* **22**(19), 1476–1478 (1997).
51. S. G. Kosinski and A. M. Vengsarkar, "Splicer-based long-period fiber gratings," in *Optical Fiber Comm. Conf., Vol. 2 of 1998 OSA Technical Digest Series*, Optical Society of America, Washington, DC, paper ThG3 (1998).
52. S. Kannan et al., "Reliability of long-period gratings," in *Optical Fiber Comm. Conf., Vol. 2 of 1998 OSA Technical Digest Series*, Optical Society of America, paper ThG6 (1998).
53. J. Jang et al., "Temperature insensitive long-period fibre gratings," *Electron. Lett.* **35**(24), 2134–2136 (1999).
54. Y. Liu, L. Zhang, and I. Bennion, "Fibre optic load sensors with high transverse strain sensitivity based on long-period gratings in B/Ge codoped fibre," *Electron. Lett.* **35**(24), 661–663 (1999).
55. H. J. Patrick, C. C. Chang, and S. T. Vohra, "Long period fibre gratings for structural bend sensing," *Electron. Lett.* **34**(18), 1773–1775 (1998).
56. J. Rathje et al., "Sensitivity of a long-period optical fiber grating bend sensor," in *Optical Fiber Comm. Conf., Vol. 2 of 1998 OSA Technical Digest Series*, Optical Society of America, Washington, DC, paper WM49 (1998).
57. H. J. Patrick and S. T. Vohra, "Directional shape sensing using bend sensitivity of long period fiber gratings," *Proc. SPIE* **3746**, 561 (1999).
58. Z. H. Chen et al., "Bent long-period fiber gratings for sensor applications," *Proc. SPIE* **3897**, 94–104 (1999).
59. C. C. Ye et al., "Bend sensing in structures using long-period optical fibre gratings," *Proc. SPIE* **4073**, 311–315 (2000).
60. J. Rathje, M. Kristensen, and J. Hübner, "Effects of fiber core concentricity error and UV illumination direction on the bend direction asymmetry of long-period gratings," in *Bragg Gratings, Photosensitivity, and Poling in Glass Waveguides*, T. Erdogan, E. Friebel, and R. Kashyap, Eds., Vol. 33 of OSA Trends in Optics and Photonics Series, Optical Society of America, Washington, DC, paper BD2 (1999).
61. Y. Liu et al., "Bend sensing by measuring the resonance splitting of long-period fiber gratings," *Opt. Commun.* **193**(1–6), 69–72 (2001).
62. Y. Q. Liu et al., "Long period fiber grating curvature sensor based on temperature-insensitive wavelength separation measurements," *Proc. SPIE* **4596**, 104–109 (2001).
63. D. A. González et al., "Spectral modelling of curved long-period fibre gratings," *Meas. Sci. Technol.* **12**(7), 786–792 (2001).
64. U. L. Block et al., "Origin of apparent resonance mode splitting in bent long-period fiber gratings," *J. Lightwave Technol.* **24**(2), 1027–1034 (2006).
65. J. Rathje and M. Kristensen, "Effects of core concentricity error on bend direction asymmetry for long-period fiber gratings," in *Bragg Gratings, Photosensitivity, and Poling in Glass Waveguides*, Optical Society of America, Washington, DC, paper SaC2 (1999).
66. H. J. Patrick, "Self-aligning, bipolar bend transducer based on long period grating written in eccentric core fibre," *Electron. Lett.* **36**(21), 1763–1764 (2000).
67. S. Michelsen, "Optical fiber grating based sensors," Ph.D. Thesis (Technical University of Denmark, Department of Communications, 2003).
68. S. Søgaard, M. Kristensen, and J. Rathje, "Characterization of a long-period grating (LPG) bend sensor in a core concentricity error fiber," in *Bragg Gratings, Photosensitivity, and Poling in Glass Waveguides, 2001 OSA Technical Digest Series*, Optical Society of America, Washington, DC, paper BTh4 (2001).
69. T. Allsop et al., "Beading and orientational characteristics of long period gratings written in D-shaped optical fiber," *IEEE Trans. Instrum. Meas.* **53**(1), 130–135 (2004).
70. D. Zhao et al., "Bend sensors with direction recognition based on long-period gratings written in D-shaped fiber," *Appl. Opt.* **43**(29), 5425–5428 (2004).

71. D. Zhao et al., "Implementation of vectorial bend sensors using long-period gratings UV-inscribed in special shape fibres," *Meas. Sci. Technol.* **15**(8), 1647–1650 (2004).
72. M. Chomat et al., "Bend sensing with long-period fiber gratings in capillaries embedded in structures," *Mater. Sci. Eng. C-Biomimetic Supramol. Syst.* **28**(5–6), 716–721 (2008).
73. M. N. Trutzel et al., "Smart sensing of aviation structures with fiber optic Bragg grating sensors," *Proc. SPIE* **3986**, 134–143 (2000).
74. R. Maaskant et al., "Fiber-optic Bragg grating sensors for bridge monitoring," *Cem. Concr. Compos.* **19**(1), 21–33 (1997).
75. M. L. Filograno et al., "Real-time monitoring of railway traffic using fiber Bragg grating sensors," *IEEE Sensors J.* **12**(1), 85–92 (2012).
76. B.-O. Guan et al., "Simultaneous strain and temperature measurement using a superstructure fiber Bragg grating," *IEEE Photonics Technol. Lett.* **12**(6), 675–677 (2000).
77. B.-O. Guan et al., "Simultaneous strain and temperature measurement using a single fibre Bragg grating," *Electron. Lett.* **36**(12), 1018–1019 (2000).
78. C. C. Ye, S. W. James, and R. P. Tatam, "Simultaneous temperature and bend sensing with long-period fiber gratings," *Opt. Lett.* **25**(14), 1007–1009 (2000).
79. C. C. Chan and B.-O. Guan et al., "Simultaneous measurement of curvature and temperature for LPG bending sensor," *Proc. SPIE* **5590**, 105–110 (2004).



**Lars Glavind** received his BEng in electronics from The Engineering College of Aarhus in 2007, and his MS in optics and electronics from Aarhus University in 2009. For one year he worked as a research engineer, with applied research projects, at Vestas Wind Systems A/S. In 2010, he started working on his PhD, regarding fiber optical blade load sensors, at the same company in cooperation with Aarhus University—Department of Engineering.

**Ib Svend Olesen** was educated as an electronic technician from Aarhus Technical School in 1981. He has since worked as a hardware and software engineer at Alarm Parts, Mita Teknik, S.P. Radio and NEG Micon. Since 2003 he has worked Vestas Wind System A/S in the sensor department.

**Bjarne Funch Skipper** received his MS in electrical engineering from Aalborg University, Denmark, in 1986. He received an industrial PhD degree in narrow linewidth lasers for coherent optical communication in 1989. He has been involved in research and development of fiber-optic telecommunication systems and is now with Aarhus School of Engineering in Denmark.

**Martin Kristensen** is a professor of photonics in the department of engineering at Aarhus University since 2004. Before this, he spent more than 10 years at the Technical University of Denmark (DTU) where he headed a group specializing in optical fiber and waveguide components. He has a long experience in design, fabrication, and characterization of optical components and has published more than 300 scientific journal and conference papers and supervised 28 PhD students. He has participated in five EU research projects and acted as work package leader in four of these.